

## Radiation Pattern Characteristics of Multiple Band-Notched Ultra Wideband Antenna with Asymmetry Slot Reconfiguration

Yusnita Rahayu

Department of Electrical Engineering  
Faculty of Engineering, University of Riau  
Pekanbaru 28293, Riau, Indonesia  
E-mail: vannebula2001@yahoo.com

Razali Ngah

Faculty of Electrical Engineering  
Universiti Teknologi Malaysia  
Johor Bahru, 81310, Malaysia  
E-mail: razalin@fke.utm.my

**Abstract-** Radiation pattern characteristics of reconfigurable asymmetry slotted ultra wideband antenna with multiple band-notched is presented. The proposed antenna is planar monopole, consisting of a microstrip feed line and modified L and U slots with a pentagonal patch on the front side and half ground plane is on the back side of the board. The measurements were conducted by using Radio Frequency measurement and instrumentation facilities, software tools available at the Wireless Communication Center in Universiti Teknologi Malaysia. The modified antennas are designed for having reconfigurable frequency notched at Fixed Wireless Access, High Performance Local Area Network, and Wireless Local Area Network. A good agreement is achieved between simulated and measured Voltage Standing Wave Ratio results. The measured result is approximately less than 2.2 over 3 GHz to 10 GHz. It was also observed that the measured radiation patterns, H-planes, are omnidirectional with a slight gain decreased at boresight direction for measuring frequencies. There are also more ripples occurred in the measured pattern compared with the simulated one. Comparison measured radiation patterns between asymmetry slotted antenna with and without notch band characteristic have been done. Multiple reflections, rotator alignment, probe rotary joint and room scattering are found as primary sources of errors that cause degradation in measured radiation patterns. Current distribution characteristic of the antenna is also reviewed.

**Keywords-** *reconfigurable antenna, slotted antenna, radiation pattern, ultra wideband, band-notched antenna.*

### I. INTRODUCTION

Reconfigurable antenna is defined as the antenna capability to reconfigure several parameters such as operating frequencies, impedance bandwidth, polarizations, and radiation patterns to fulfill operating requirements. The development of this antenna poses significant challenges to both antenna and system designers. The challenges lie not only in obtaining the desired level of antenna functionality but also in integrating this functionality into complete systems to arrive at efficient and cost effective solution.

This section reviews the concept of reconfigurable antennas that reuse their entire geometry for band-notched frequency Applications. Paper [1] is taken as a reference paper for this extension works. The concept is that each operating band resonates on the portion of the entire antenna geometry, therefore there is almost no extra size required to

create multiband characteristics. A frequency shift can be achieved by connecting or disconnecting one or more antenna elements. Every configuration of an antenna will have a different resonating frequency and different radiation pattern. An antenna has to be designed with the objective that it should exhibit banding-notched behaviour and has to be compact. Various techniques used have been reported in literature [1][2][3][4][5][6][7][8][9][10][11][12][13][14][15].

In [2], there are two varieties of slotted antennas which have a frequency notched reported, a triangular notch and elliptical notch. Both antennas have frequency notch characteristics where the arc length of slots form a half wavelength resonance structure of particular frequencies, thus a destructive interference takes place causing the antennas to be non-responsive at that frequency. Other types of this kind antenna was reported in [5], a band-notched UWB (ultra wideband) antenna using a slot-type SRR (split ring resonator) was found very effective in rejecting unwanted frequency, such as that for WLAN (Wireless Local Area Network) service, in terms of its selectivity and small dimension. The SRR is composed of two concentric split ring slots and proposed for band stop application, since it provides a high Q characteristic. The slotted SRR was positioned near the feeding point to provide more coupling with the field. A multiple band-notched planar monopole antenna using multiple U-shape slots for multi band wireless system was also presented in [6]. The half wavelength U-shape slots were symmetrically inserted in the center of the planar element. In order to generate the two bands-notched characteristics, three U-shape slots were proposed.

The notch bands were also obtained by inserting an L-shaped slot in the ground plane [13]. The proposed antenna was fed by CPW (coplanar waveguide). By altering the length of the L-shaped slot, it can easily adjust the notched frequency. The similar techniques were also proposed in [14], the reject frequency was obtained by cutting a rectangular slot in the CPW ground which reduces the potential interference between UWB systems and the narrow systems. Thus, it is found that the use of slots for a patch or ground plane significantly provide band-notched characteristics.

An alternative antenna design without using the slot to obtain band-notched characteristic was proposed in [7]. The antenna consists of two same size monopoles and a small strip bar at the center showing the band rejection

performance in the desired frequency bands. The use of strip bar leads to high impedance at the notch frequency. The total length of strip bar from the ground plane is equal to a quarter-wavelength at the notch frequency.

In this paper, novel reconfigurable UWB antennas are designed by adopting the half wavelength slot structure technique. This technique has been found and proven in [2][5][6][13][14] as a very effective technique in providing band-notched characteristics. This paper mainly focuses on the reconfigurable notch band through the introduction of new slots, L and U slots, on the pentagonal patch antenna. This asymmetry couple slot, L and U, creates a new novelty slot design. Most published papers use a uniform and symmetry slot structure for their antenna design. In this paper, it is shown that the asymmetry slots can be designed to form band-notched characteristics with comparable results to others. This slot structure chosen is mostly influenced by current distribution surrounding the antenna patch.

Section II will discuss the antenna geometry and its current distribution characteristics. The techniques to design new reconfigurable slotted antennas having band-notched frequencies are also presented. The band-notched operation is achieved by incorporating some small gaps instead of pin diodes into the slot antenna. The term of small gaps in this paper will refer to switches. The switches are used to short the slot in pre-selected positions along the circumference. The length of the slot antenna can be lengthened or shorted by closing or opening the switches, allowing for a change in the notched frequency. Then the performances of reconfigurable antennas, in terms of the VSWR (voltage standing wave ratio) and radiation patterns, will be discussed and evaluated in Section III. Comparison measured radiation patterns between slotted antenna with and without band-notched characteristic is also discussed. Errors in measured radiation patterns are further analyzed and presented. Finally, a conclusion will be given in Section IV.

## II. ANTENNA DESIGN

Fig. 1 shows the proposed antenna structure printed on the FR4 substrate of  $\epsilon_r = 4.6$ . The pentagonal antenna is vertically installed above a ground plane ( $l_{\text{grd}}$ ) of 11 mm. The optimum feed gap ( $h$ ) to the ground plane is found to be 1.5 mm. The dimension of substrate is chosen to be  $30 \times 30 \text{ mm}^2$  ( $W_{\text{sub}} \times L_{\text{sub}}$ ) in this study. The antenna has a pentagonal patch with a width ( $w$ ) of 15 mm and a length ( $l$ ) of 12 mm. This shape is as a variety of rectangular shape with bevel techniques. This antenna geometry is similar to the antenna geometry presented in [1].

The slots proposed on patch effectively change its electrical length over a very wide bandwidth. Slot dimensions of the proposed antenna are listed in Table 1. The slot width is 0.5 mm in order to improve the bandwidth above 10 GHz. Asymmetry slot design, L and U, on this proposed antenna results novelty structure of the slotted UWB antenna, this is as one of contribution in this paper.

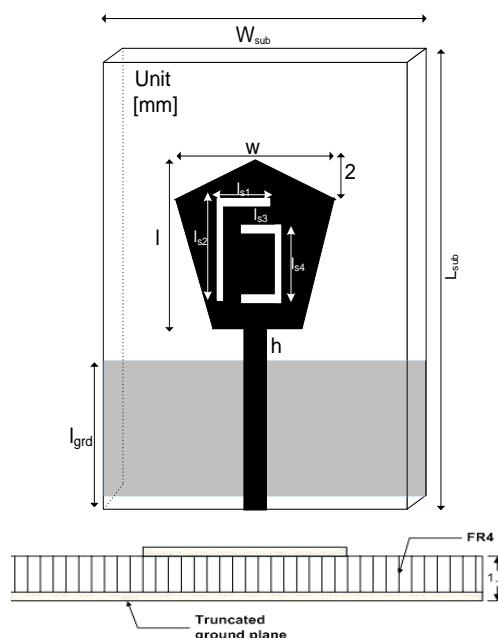


Figure 1. Geometry of L and U slotted antenna

TABLE I. DIMENSION OF L AND U SLOT

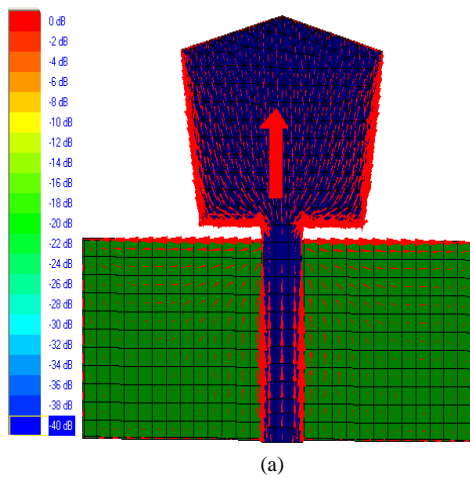
Description	L and U Slots	
	Symbol	Size [mm]
Slot length	Is1	6
	Is2	9
	Is3	3
	Is4	6.5

### A. Current Distribution Characteristics

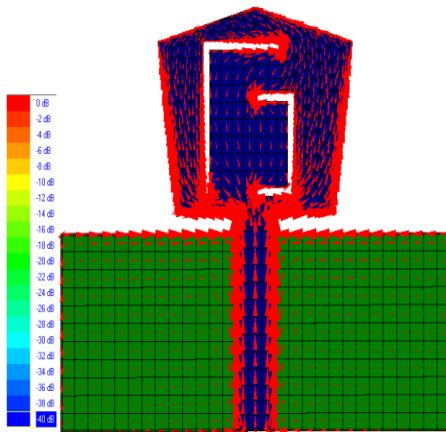
The geometry of the antenna implies the current courses and makes it possible to identify the active zone in the antenna. Active zone is the matching and radiator zone. Acting on matching and radiating areas allows controlling the bandwidth [12].

The couple slots, L and U, are designed very carefully by studying the current flow distribution which will give input impedance improvement. The study of the current distribution for bandwidth enhancement has been conducted in [16]. The current flows on a planar monopole antenna reveals that it is mostly concentrated in the vertical and horizontal edges as shown in Fig. 2(a). The current distribution on patch surface is disturbed by the introduction of new slots, L and U, as presented in Fig. 2(b).

It is observed that the horizontal current distributions are focused on the bottom edge of pentagonal patch. The discontinuity occurred from beveling at the bottom side of the patch and has enforced the excitation of vertical current mode in the structure, which presents a very wide bandwidth.



(a)



(b)

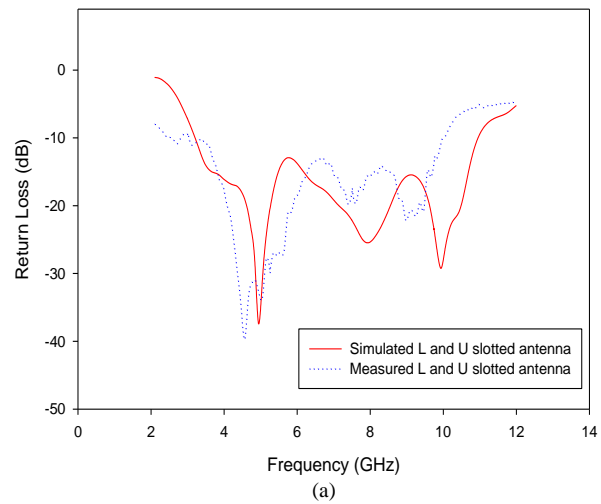
Figure 2. Current distribution characteristics

From Fig. 2(b), the current distribution is less of the area between both slots. However, these slots have resulted more vertical currents flowing to the patch. The U slot is designed to improve the upper dip resonance and the L slot improves the lower dip resonance. Individual L and U slot current distribution with their simulated results was reviewed in [17]. The coupling both slots has shown a good return loss with respect to -10 dB over UWB frequency range as presented in Fig. 3(a).

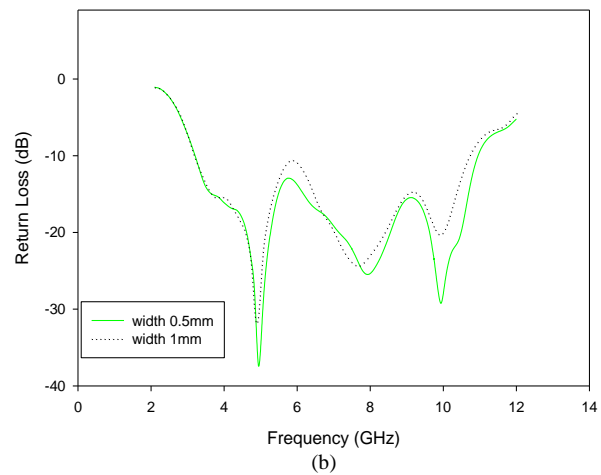
#### B. Simulated and Measured Return Loss

The simulated and measured return loss is presented in Fig. 3(a). The measured return loss is slightly shifted to the simulated one, but they still cover 2.5 GHz to 10.1 GHz as what the UWB required. The length of L slot is 14.5 mm approximately equal to  $0.25\lambda$  at 5.3 GHz, and the length of U slot is 11.5 mm approximately equal to  $0.4\lambda$  at 10.3 GHz.

It is also observed that the width of slots chosen affect to the return loss of dip resonance especially at an upper frequency as shown in Fig. 3(b). The width of 0.5 mm results -28 dB of return loss at 10.3 GHz.



(a)



(b)

Figure 3. Simulated and measured return loss

This measurement was done by using a 50- $\Omega$  SMA connector which is soldered at the bottom edge of microstrip line and connected to the network analyzer by an RF (Radio Frequency) cable. The RF cable significantly affects the performance of the AUT (antenna under test). However, some differences in the simulated and measured results are expected, since in the simulation model the mismatch due to the adapter and connector used are not taken into consideration. In reality the coaxial cable has a considerable effect, especially the length of its inner conductor, which is connected to the input of the antenna, creating an additional inductance. In addition, since the antenna is fed by a microstrip line, misalignment can result because etching is required on both sides of the dielectric substrate. The alignment error results degradation to the antenna performance.

### C. Reconfigurable Techniques

As mentioned in Section 1, the half wavelength slot structure technique is used in designing the proposed UWB slotted antenna. The main purpose here is how to design the reconfigurable UWB slotted antenna without major modification from the previous antenna design presented in [16][17]. The unique of this proposed reconfigurable UWB antenna is the antenna has additional ability in rejecting the FWA (Fixed Wireless Access) band, whereas most existing papers focusing in rejecting WLAN and HIPERLAN (High Performance Local Area Network) bands. Licensed band at FWA for point to multipoint radio systems assigned by MCMC (Malaysian Communications and Multimedia Commissions) for 3.4 to 3.7 GHz is considered giving potential interference to UWB application. This is due to the allocation frequency for this FWA within the UWB range. Therefore, recently the consideration of UWB antennas is not only focused on an extremely wide frequency bandwidth, but on the ability of rejecting the interference from WLAN 11.a (5725–5825 MHz) and HIPERLAN (5150–5350 MHz) within the same propagation environment. Thus, the proposed notched antenna is not only designed to reject interference from WLAN, HIPERLAN but also from FWA.

The basic geometry of L and U slotted antenna will be taken as a reference to form a new modified L and U reconfigurable slotted antennas. There are maximum six switches used to provide the reconfigurable function. No especial matching network is used and the matching properties are solely determined by the placement of the switches. The number of switches used and their placement are based on the notched band required. The on-off switches will determine the total slot length at a certain notched band. With the notched band characteristic, the antenna allows to reconfigurable its frequency that only responds to other frequencies beyond the rejection bands within the UWB bandwidth. However, the dimensions of the antenna and substrate are kept equal to the original model.

For the simulation purposed, the switches are considered as ideal switches and are modeled as small patches that connect or disconnect the adjacent slot, changing the antenna's slot length.

In Fig. 4, the switches have different colors for on and off state condition. Blue color represents the on state condition and red color for the off state condition. In order to provide the UWB characteristic, the switches are placed as shown in Fig. 4(a). Three switches of #2, #3, and #4 are in the off state position. Other switches of #1, #5, and #6 are in the on state condition. When the switches are in the off state condition, the gap between slots occurs and the current flowing to the gap. When the switches are in the on state condition, there is no current flowing to the slots. Thus it forms continuous slots. The switches of #2 and #3 are incorporated to the first additional slot ( $I_{s20}$ ) which is 3.5 mm of slot length. The switch of #4 is attached to the second additional slot ( $I_{s21}$ ) which is 2.5 mm of slot length. The two additional slot lengths,  $I_{s20}$  and  $I_{s21}$ , are very critically determined by the frequency notched band characteristics.

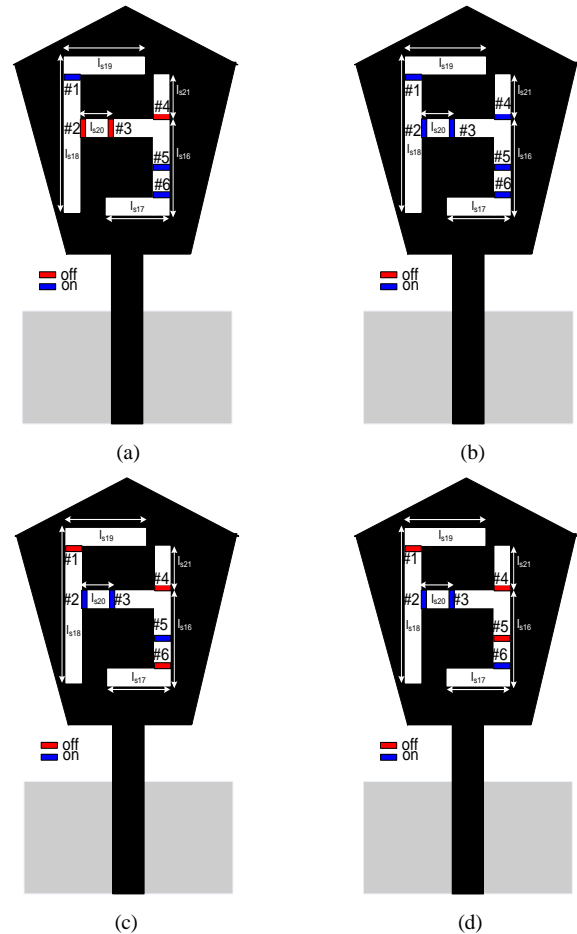


Figure 4. Switching configuration for L and U slotted antennas: (a) without notched, (b) notched at FWA, (c) notched at HIPERLAN, (d) notched at WLAN

To accommodate the notch frequency at FWA band, the length of U slot is lengthened than the previous model. Thus, six switches are used and placed systematically. The frequency notched characteristic antenna at FWA is shown in Fig. 4(b). All switches are in the on state position (continuous slot). Total slot lengths are 32 mm or approximately equal to  $0.4\lambda$  at 3.7 GHz. The total slot lengths mean the sum of slot lengths of L, U and additional slots. Fig. 4(c) and Fig. 4(d) present the frequency notched characteristic antenna at HIPERLAN and WLAN, respectively. To reject interference from HIPERLAN, the switches of #1, #4, and #6 are in the off state position while switches of #2, #3, and #5 are in the on state position. It is investigated that by inserting those switches in the off state condition broke the connection between slots. This break connection has reduced the slot length to be 20.75 mm or approximately equal to  $0.33\lambda$  at 5.2 GHz. Thus, the antenna has a frequency notched at HIPERLAN. The total slot length is measured by the length of connecting slots.

The configuration of switches in Fig. 4(d) have resulted an antenna with frequency notched at WLAN. It is shown that the switch of #5 is set in the off state position in order to reduce the slot length, while the switch of #6 is set in the on

state position. This is the only difference while comparing to the HIPERLAN configuration. Total slot lengths are 18 mm or approximately equal to  $0.33\lambda$  at 5.75 GHz and measured by the length of connecting slots.

For prototype development, the gaps are created in the UWB antenna pattern, which are represented as switches. The dimensions of switches used in these prototypes are  $0.7\text{ mm} \times 1\text{ mm}$ . Although this model is ideal, it gives a good approximation for the commercial pin diode switches. The photograph of the antenna prototype that has a band-notched at FWA is shown in Fig. 5.

### III. EXPERIMENTAL VERIFICATION

Fig. 6 shows the simulated and measured VSWR for reconfigurable modified L and U slotted antennas. By varying the slot lengths and break the connection between slots using switches, the proposed frequency notched is achieved.

The simulated results show the FWA notched band obtained from 3.57 GHz to 3.86 GHz with the total slot length of 32 mm at 3.7 GHz, which is the center frequency. While the HIPERLAN and WLAN notched bands are from 4.84 GHz to 5.33 GHz and 5.53 GHz to 6.02 GHz, respectively. It is noted that beyond the frequency notched bands, the VSWR is kept to be less than 2.

The measured VSWR is approximately less than 2.2 over 3 GHz to 10 GHz, except for the antenna with band-notched at HIPERLAN band. The VSWR beyond 9.5 GHz is getting worse. For band-notched at FWA, the rejection is in the range of 3.76 GHz to 4.25 GHz, and the rejection of HIPERLAN is 5.23 GHz to 5.53 GHz. The antenna with band-notched at WLAN band has the rejection in the range of 5.72 GHz to 6.1 GHz. Even though the band-notched slightly shifted from the required bands, but it still covers the rejection bandwidth.

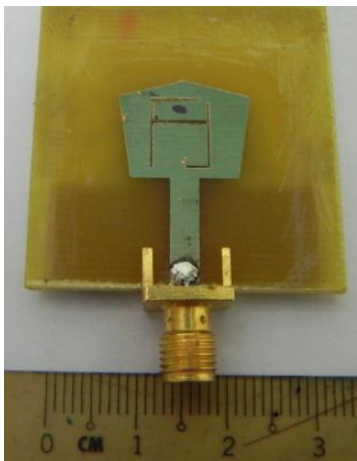
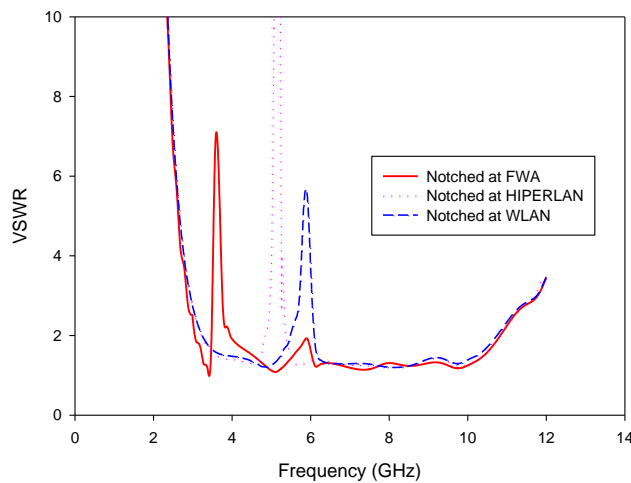
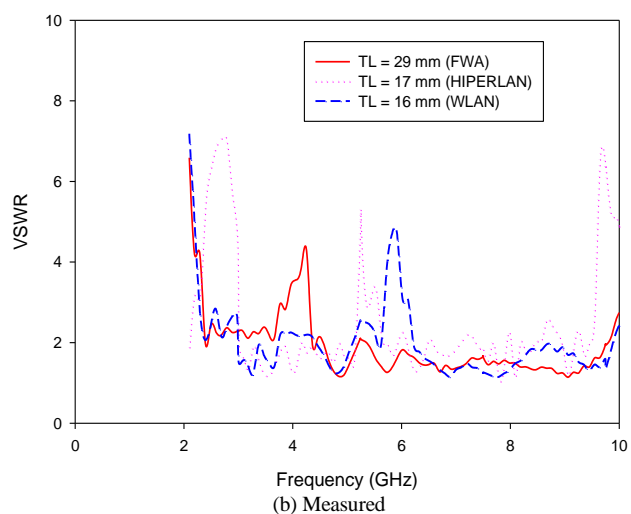


Figure 5. Photograph of FWA notch band antenna



(a) Simulated



(b) Measured

Figure 6. Simulated and measured VSWR for reconfigurable modified L and U slotted antennas

#### A. Spherical Near-Field Testing

Once the resonance frequencies were identified, principal radiation patterns were taken to characterize the operational performance of each antenna. These measurements were obtained using the indoor anechoic chamber room. For these measurements, the chamber was arranged as shown in Fig. 7.

From Fig. 7, it shows the measurement setup for both antenna and probe which were mounted to the vertical positioned-holders. The probes available at the chamber are in the frequency ranges of 3.95 – 5.85 GHz and 8.95 – 12 GHz, respectively.

The existing chamber employed the spherical near-field measurement. By definition, near-field tests are done by sampling the field very close to the antenna on a known surface. From the phase and amplitude data collected, the

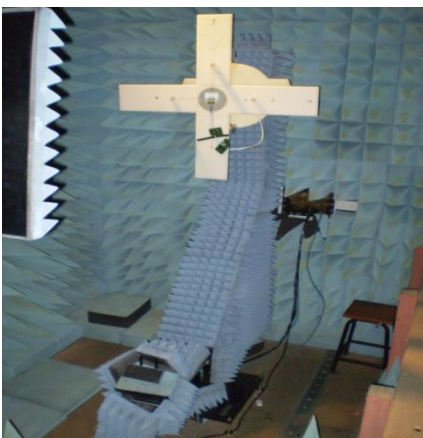
far-field pattern must be computed in much the same fashion that theoretical patterns are computed from theoretical field distributions. The transformation used in the computation depends on the shape of the surface over which the measurements are taken with the scanning probe [18].

This spherical system acquired a double data set on the AUT. The '360phi' data set is taken with full  $360^\circ$  phi rotation of the AUT, but with only  $0^\circ - 180^\circ$  motion in theta. In this mode, the AUT's Z axis will only be looking at one side of the chamber during the measurement [19]. The AUT was swept every  $2^\circ$  increment in the azimuth plane in order to reduce the aliasing errors. Data point spacing aliasing errors will occur for spherical near-field measurements if the data point spacing is not small enough to sample the highest spatial frequency components in the measured data [19].

The radiation patterns were measured at 4 GHz and 5.8 GHz. The measured radiation patterns were plotted into H (horizontal) and V (vertical) cuts. The H-cut is cut for the azimuth plane with the fixed elevation angle at  $0^\circ$  and vary the azimuth angle. The V-cut is cut for the elevation plane with a fixed azimuth angle at  $0^\circ$  and vary the elevation angle.



(a)



(b)

Figure 7. The radiation pattern measurement setup inside the anechoic chamber room

### B. Radiation Pattern Measurement

Radiation pattern's measurements have been done for both proposed antennas with and without band-notched characteristic. Fig. 8 and Fig. 9 show the radiation pattern results at 4 GHz and 5.8 GHz for antenna without band-notched characteristic, respectively.

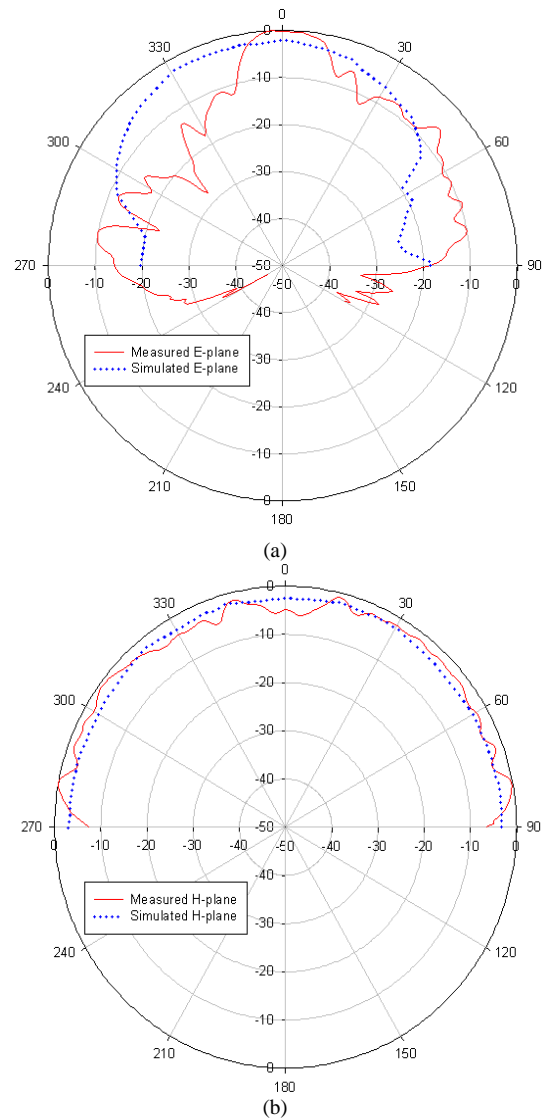


Figure 8. Simulated and measured E and H-planes for the slotted antenna at 4 GHz (without notched band)

All radiation patterns were measured and examined for both E and H-planes. They show acceptable results where the overall H-planes for both frequencies providing omnidirectional patterns. But, the more ripples occur in the measured E-planes radiation pattern. This is due to some errors during the measurement process.

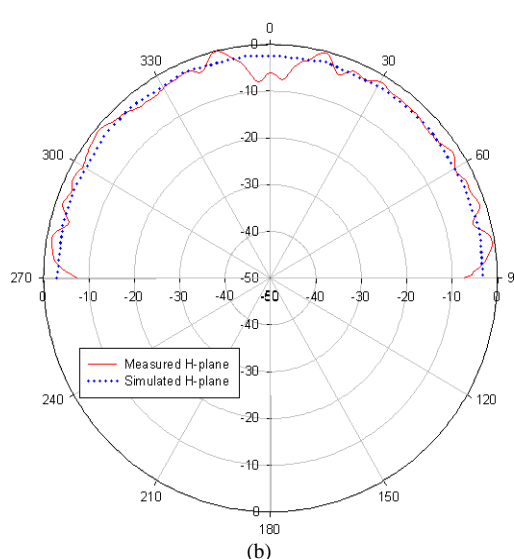
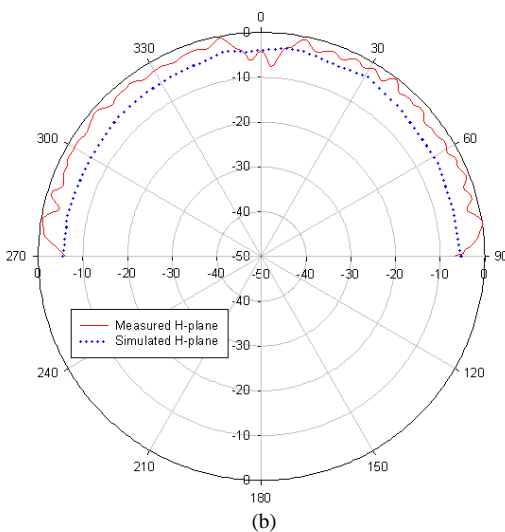
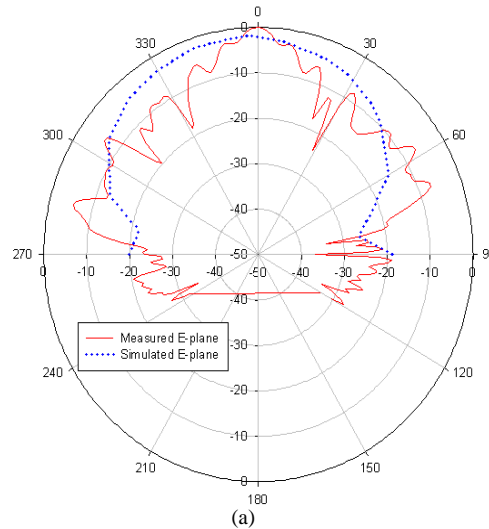
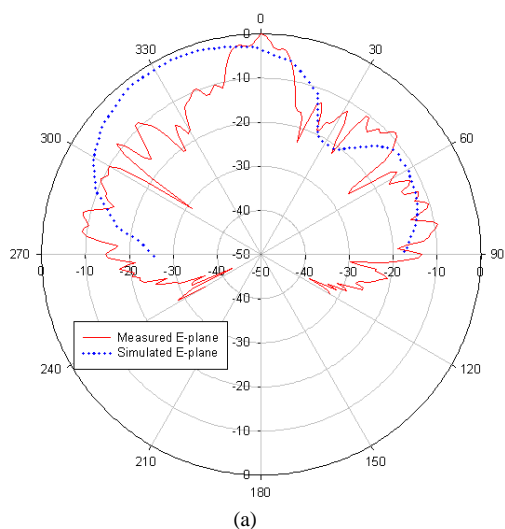


Figure 9. Simulated and measured E and H-planes for the slotted antenna at 5.8 GHz (without notched band)

Figure 10. Simulated and measured E and H-planes at 4 GHz for antenna notched at FWA

Measured and simulated radiation patterns of reconfigurable antennas with band-notched characteristic are plotted in Fig. 10 to Fig. 15. Comparison radiation patterns for both proposed antennas have been done. From the results obtained, all H-plane patterns show nearly similar patterns, omnidirectional, for all measured frequencies. But, the E-plane patterns show the variation patterns for each frequency.

Fig. 10 and Fig. 11 show the radiation patterns of antenna notched at FWA for 4 GHz and 5.8 GHz, respectively. From both figures, there are slightly backlobes present for the E-planes. Both H-planes are omnidirectional with a slight gain decreased at boresight direction. The H-planes patterns retain a satisfactory omnidirectionality (less than 10 dB gain variation in most directions) over the entire bandwidth in both simulation and experimental.

The E-plane pattern is the radiation pattern measured in a plane containing feed, and the H-plane pattern is the radiation pattern in a plane orthogonal to the E-plane.

The results show that the radiation patterns are changing as the frequency increases. The patterns resulted from the measurements have many ripples in amplitude due to many reflections into the field between the AUT and probe. The reflections may come from the room (floor and ceiling), chamber scattering, antenna holder itself and track inside the anechoic chamber. It is shown in previous Fig. 7, the antenna size is very small compared to its huge holder, and also the floor and the track surrounding the antenna tower are not all covered by absorber.

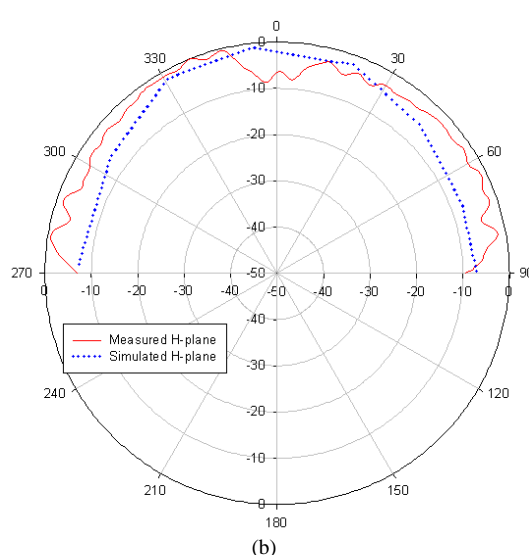
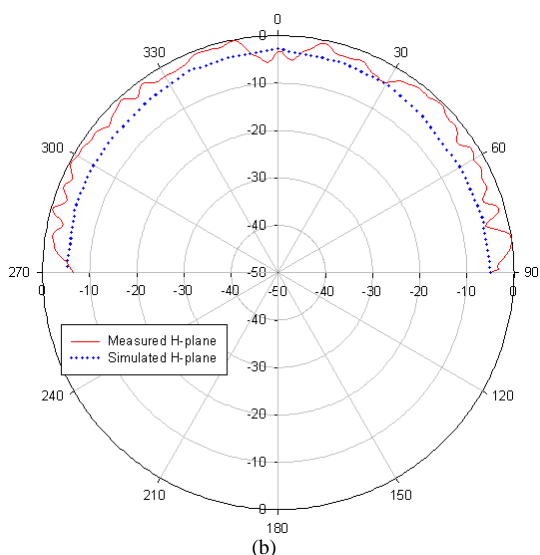
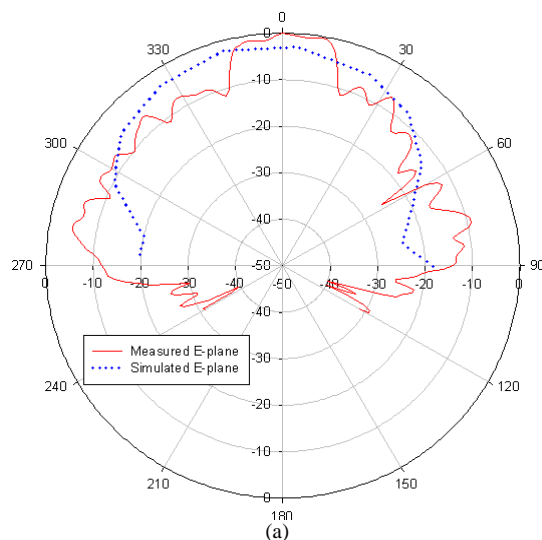
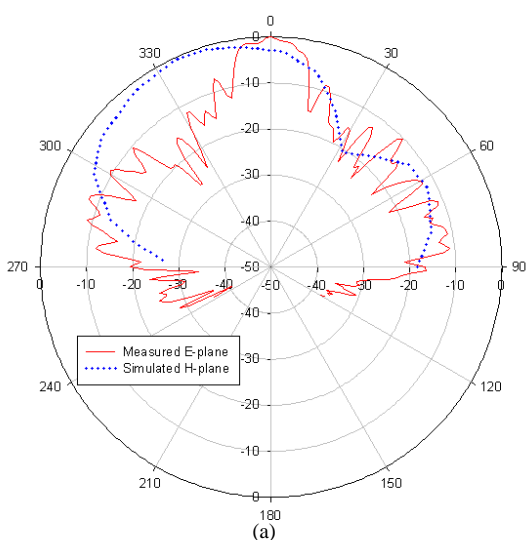


Figure 11. Simulated and measured E and H-planes at 5.8 GHz for antenna notched at FWA

Figure 12. Simulated and measured E and H-planes at 4 GHz for antenna notched at HIPERLAN

Fig. 12 to Fig. 15 shows the radiation patterns for antenna notched at HIPERLAN and WLAN. The E and H-planes are measured at 4 GHz and 5.8 GHz for both testing.

It is observed that the measured E-planes for antenna notched at HIPERLAN broader than the measured E-planes for antenna notched at FWA. However, the patterns resulted from the measurement are still having many ripples in amplitude. Due to the track surrounding the antenna tower are not all covered by absorber, if moved sideways about half cycle the ripples occur and if moved vertically the ceiling and floor reflections are indicated. The most significant is probably from improper cable connectors allowing excitation of the outside surface [18]. Leakage will be added to the measured pattern as degradation. Both H-planes are omnidirectional.

The measured radiation patterns demonstrate that at the low end of the operating band, the currents are well distributed over the patch antenna plate so the patterns are relatively broad. But at the high end of the operating band, the currents are concentrated near the slot, thus the fields radiate mainly through the slot.



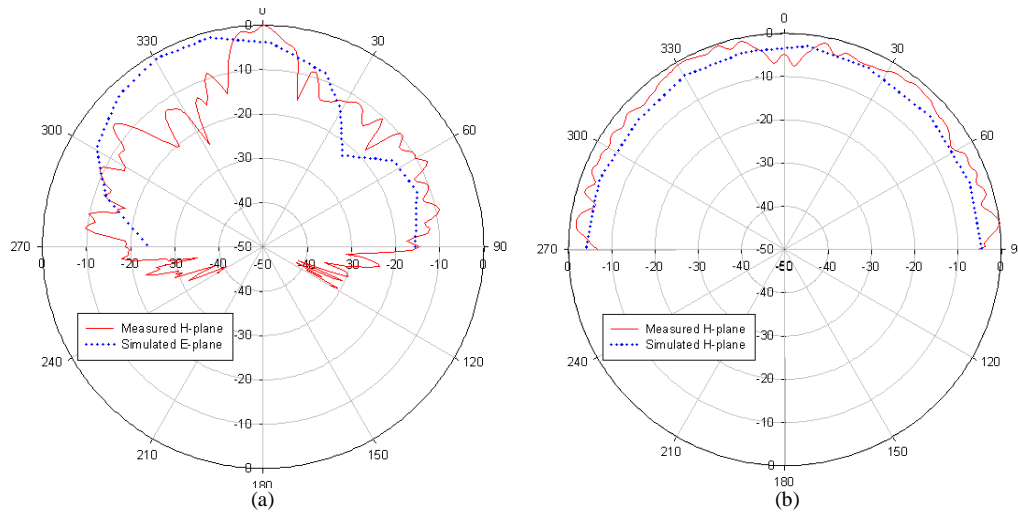


Figure 13. Simulated and measured E and H-planes at 5.8 GHz for antenna notched at HIPERLAN

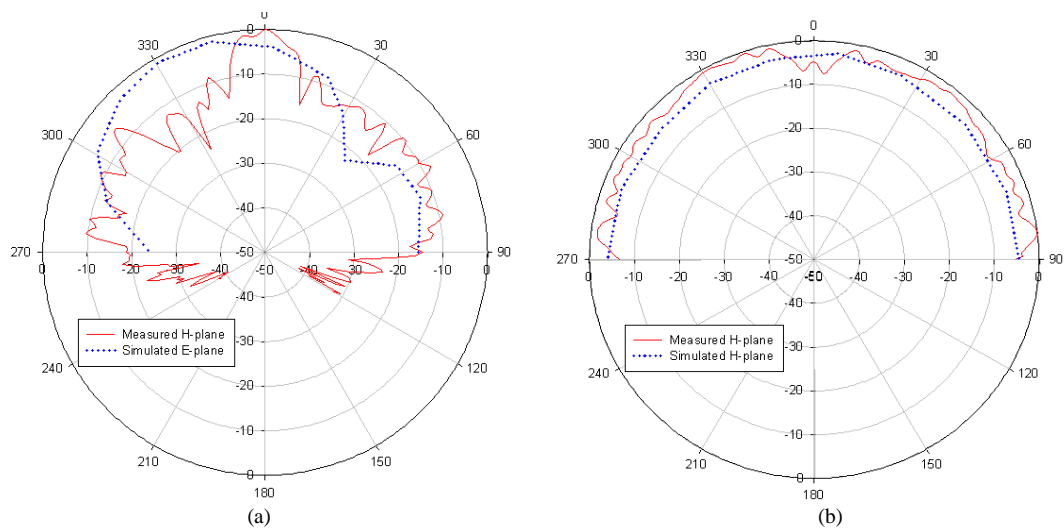


Figure 14. Simulated and measured E and H-planes at 4 GHz for antenna notched at WLAN

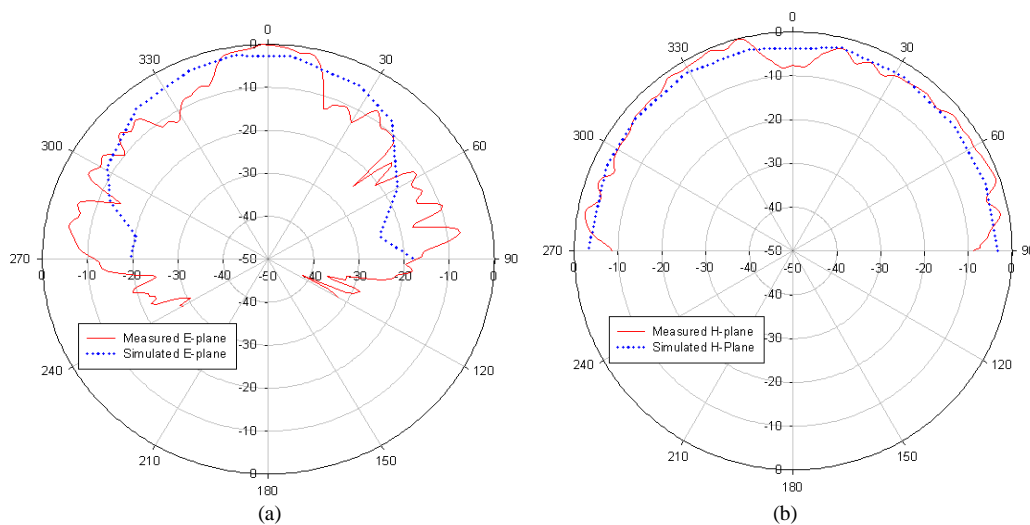


Figure 15. Simulated and measured E and H-planes at 5.8 GHz for antenna notched at WLAN

### C. Estimating Error Analysis in Radiation Pattern Measurement

Since the measured radiation patterns obtained have many ripples and dips for the E-planes, the error analysis have been done to estimate the uncertainty and the caused of the error. The development of analysis and measurements to estimate the error during measurement in spherical near-field has been conducted in [19] [20].

During measurement process, several requirements are needed to take into consideration. It is observed that multiple reflections, rotator alignment, probe rotary joint and room scattering are shown as primary sources of errors that cause degradation in measured radiation pattern. Multiple reflections between AUT and probe produce the ripple in the measured data. The correction is difficult to do due to the need a series of near-field measurement at Z-positions separated by  $\lambda/8$ . The far-fields are then calculated for each and averaged [21]. In the case of multiple reflections and random errors, multiple measurements are required.

Fig. 16 shows the example of the random errors presented during measurement. These measured patterns are from repeated measurement at 5.8 GHz for L and U slotted antenna. Some corrections on the AUT alignments have also been done. From the pattern comparison graphics show the random error occurs in amplitude and phase during multiple measurements.

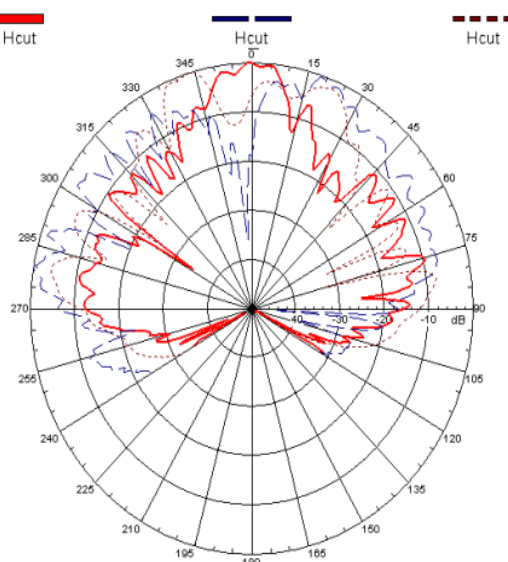


Figure 16. An example of results of random errors for L and U slotted antenna at 5.8 GHz

When the AUT is not precisely aligned to reference coordinate system, vector components or coordinate angles may change for some rotation. This correction can be done by realigning the AUT position.

The rotator alignment for spherical is a special case of position errors. The orthogonally and intersection of the theta and phi axes and the coincidence of the phi and probe

polarization axes can be checked by measuring and comparing near-field cuts at  $\theta = 0$  and 180 degrees. The misalignment can be corrected by adjustments of the mechanical system. However, the difference values still present at those near-field cuts of measured data.

The probe rotary joints associated with the theta and phi rotators produce some amplitude and phase variations as it is moved and this is as a function of theta and phi. The error can be observed from the measured data by comparing the amplitudes and phases of the two components at  $(\theta, \phi)$  coordinates,  $(0, 0)$  and  $(0, 180)$  [20]. At these points, the amplitude should be identical and the phases should be either identical or 180 degrees different. This error is more important at high frequencies where rotary joints may not be as accurate. From the measured data obtained, it is observed that the variations have presented in amplitudes and phases for those points of both proposed antennas. Thus, this error contributes to the uncertainty in far-field results.

Both probe and room scattering can produce higher spatial frequencies in the data. The smaller data point spacing is needed to avoid the aliasing errors. The room scattering effect can be more severe when low gain AUT's are being measured [20]. In this measurement, the  $2^\circ$  data point spacing is used for scanner movement. Scattering from structures and absorber introduces an error that is difficult to estimate. This is because the procedure is demanding and time consuming. The AUT and probe must be translated together in a combination of X, Y and Z movements while maintaining precise angular alignment. The translations should be at least multiple wavelengths in dimension and the AUT must be realigned in the new position. Comparison of the patterns from the two locations provides an estimate of the room scattering but it is difficult to distinguish from alignment differences, probe/AUT multiple reflections and system drift [20].

It is concluded that obtaining true patterns depends primarily on accurately positioning the probe, accurately measuring the field, and eliminating distortions in the field introduced by the room, tracks, or probe. The room reflections must be lower than the basic side-lobes level and the probe must have low reflections. The probe position must be accurate to give better tolerance corresponding to the side-lobe level. In a spherical near-field range, the spherical measurement surface will be imperfect due to inaccuracies of the positioners and misalignment of these positioners [19].

## IV. CONCLUSION

Novel reconfigurable asymmetry slotted antennas with band-notched characteristic at FWA, HIPERLAN, and WLAN band have been successfully designed and developed. The measured VSWR less than 2.2 is achieved. The radiation pattern behaviour for both proposed antennas with and without band-notched characteristic has been examined. The omnidirectional patterns are obtained for all measured H-plane patterns at 4 GHz and 5.8 GHz for both antennas. The E-plane patterns show a unique pattern for each frequency. It tends to radiate broadly in all directions but more ripples occur due to some errors during the

measurement process. Current distribution characteristic for the asymmetry slotted antenna is presented as well. It is shown that the introduction of asymmetry slots has disturbed the current flow on pentagonal patch. Six switches are attached to the antenna for reconfigurable purpose. By varying the slot length, the frequency notched antennas are performed at certain frequencies. Errors in measured radiation patterns are further analyzed. It is concluded that several requirements need to take into consideration during measurement process such as rotator alignment, room scattering and probe rotary joint.

#### ACKNOWLEDGEMENT

The authors would like to thank the Wireless Communication Center (WCC) of Universiti Teknologi Malaysia for their supporting and facilitating this research.

#### REFERENCES

- [1] Yusnita Rahayu, Azlyna Senawi, and Razali Ngah, "Radiation Pattern Behaviour of Reconfigurable Asymmetry Slotted Ultra Wideband Antenna," Proc. The Seventh International Conference on Wireless and Mobile Communications (ICWMC 2011), June. 2011, pp. 81-86, ISBN: 978-1-61208-140-3.
- [2] H. G. Schant, G. Wolenc, and E. M. Myszka, "Frequency Notched UWB Antenna," Proc. IEEE Conference on Ultra Wideband Systems and Technologies (UWBST), Nov. 2003, pp. 214-218, doi: 19.1109/UWBST.2003.1267835.
- [3] Yongjin Kim and Do-Hoon Kwon, "CPW-Fed Planar Ultra-Wideband Antenna Having a Frequency Band Notch Function," Electronics Letters, vol. 40(7), April. 2004, pp. 403-405, doi: 10.1049/el:20040302.
- [4] Saou-Wen Su, Kin-Lu Wong, and Fa-Shian Chang, "Compact Printed Ultra-Wideband Slot Antenna with a Band Notched Operation," Microwave & Optical Technology Letters, vol. 45(2), April. 2005, pp. 128-130, doi: 10.1002/mop.20746.
- [5] J. Kim, C. S. Cho, and J. W. Lee, "5.2 GHz Notched Ultra-Wideband Antenna Using Slot-type SRR," Electronics Letters, vol. 42(6), March. 2007, pp. 315-316, doi: 10.1049/el:20063713.
- [6] Wang-Sang Lee, W. G. Lim, and Jong-Won Yu, "Multiple Band-Notched Planar Monopole Antenna for Multiband Wireless Systems," IEEE Microwave and Wireless Components Letters, vol. 15(9), Sept. 2005, pp. 576-578, doi: 10.1109/LMWC.2005.855374.
- [7] Seokjin Hong, Kyungho Chung, and Jaehoon Choi, "Design of a Band-Notched Wideband Antenna for UWB Applications," Proc. IEEE Antennas and Propagation Society International Symposium, July. 2006, pp. 1709-1712, doi: 10.1109/APS.2006.1710892.
- [8] K. C. L. Chan and Yi Huang, "A Compact Semi-Circular Disk Dipole with Notched Band for UWB Applications," Proc. The Institution of Engineering and Technology Seminar on Ultra Wideband Systems, Technologies, and Applications, April. 2006, pp. 226-230, ISBN: 0-86341-625-X.
- [9] Kyungho Chung, Jaemoung Kim, and Jaehoon Choi, "Wideband Microstrip-Fed Monopole Antenna Having Frequency Band Notch Function," IEEE Microwave and Wireless Components Letters, vol. 15(11), Nov. 2005, pp. 766-768, doi: 10.1109/LMWC.2005.858969.
- [10] Yongjin Kim and Do-Hoon Kwon, "Planar Ultra Wideband Slot Antenna with Frequency Band Notch Function," Proc. IEEE Antennas and Propagation Society International Symposium, vol. 2, June. 2004, pp. 1788-1791, doi: 10.1109/APS.2004.1330545.
- [11] Tamer Aboufoul and Akram Alomainy, "Reconfigurable Printed UWB Circular Disc Monopole Antenna," Proc. IEEE Loughborough Antennas & Propagation Conference (LAPC), Nov. 2011, pp. 1-4, doi: 10.1109/LAPC.2011.6114078.
- [12] I. Pele, Y. Mahe, A. Chousseaud, S. Toutain, and P. Y. Garel, "Antenna Design with Control of Radiation Pattern and Frequency Bandwidth," Proc. IEEE Antennas and Propagation Society International Symposium, vol. 1, June. 2004, pp. 783-786, doi: 10.1109/APS.2004.1329787.
- [13] Luyang Ji, Guang Fu, Jiayue Zhao, and Qiyilu, "CPW-fed UWB Antenna with the Design of Controlable Band Notch," Proc. IEEE International Conference on Electronics, Communications and Control (ICECC), Sept. 2011, pp. 788 - 790, doi: 10.1109/ICECC.2011.6067554.
- [14] Henan Wang and Ying Song Li, "Bandwidth Enhancement of A Wide Slot UWB Antenna with A Notch Band Characteristic," Proc. IEEE 3<sup>rd</sup> International Conference on Communication Software and Networks (ICCSN), May. 2011, pp. 365-368, doi: 10.1109/ICCSN.2011.6014070.
- [15] R. Movahedinia, M. Ojaroudi, and S. S. Madani, "Small Modified Monopole Antenna for Ultra-Wideband Application with Desired Frequency Band-Notch Function," IET Microwaves, Antennas & Propagation, Aug. 2011, vol. 5(11), pp. 1380-1385, doi: 10.1049/iet-map.2009.0560.
- [16] Yusnita Rahayu, Tharek Abd. Rahman, Razali Ngah, P. S. Hall, Numerical Analysis of Small Slotted Ultra Wideband Antenna Based on Current Distribution for Bandwidth Enhancement, Ultra-Wideband, Short Pulse Electromagnetics 9 (UWB SP 9), 2010, Springer Publication, Part 4, pp. 215-223, doi: 10.1007/978-0-387-77845-7\_25.
- [17] Yusnita Rahayu, Tharek Abd. Rahman, Razali Ngah, P. S. Hall, "Small Printed Ultra Wideband Antenna with Having A Coupled Slot," Proc. IEEE Loughborough Antennas & Propagation Conference (LAPC), Nov. 2009, pp. 397-400, doi: 10.1109/LAPC.2009.5352426.
- [18] Gary E. Evans, Antenna Measurement Techniques, Boston, London: Artech House. 1990.
- [19] G. Hindman and Allen C. Newell, "Simplified Spherical Near-Field Accuracy Assessment," Technical Paper, Nearfield System, Inc. 2004.
- [20] Allen Newell and Greg Hindman, "Planar and Spherical Near-Field Range Comparison with -60 dB Residual Error Level," Technical Paper, Nearfield System, Inc. 2004.
- [21] E. Antonino-Daviu, M. Cabedo-Fabres, M. Ferrando-Bataller, and A. Valero-Nogueira, "Wideband Double-Fed Planar Monopole Antennas," Electronics Letter, vol. 39(23), Nov. 2003, pp. 1635-1636, doi: 10.1049/el:20031087.